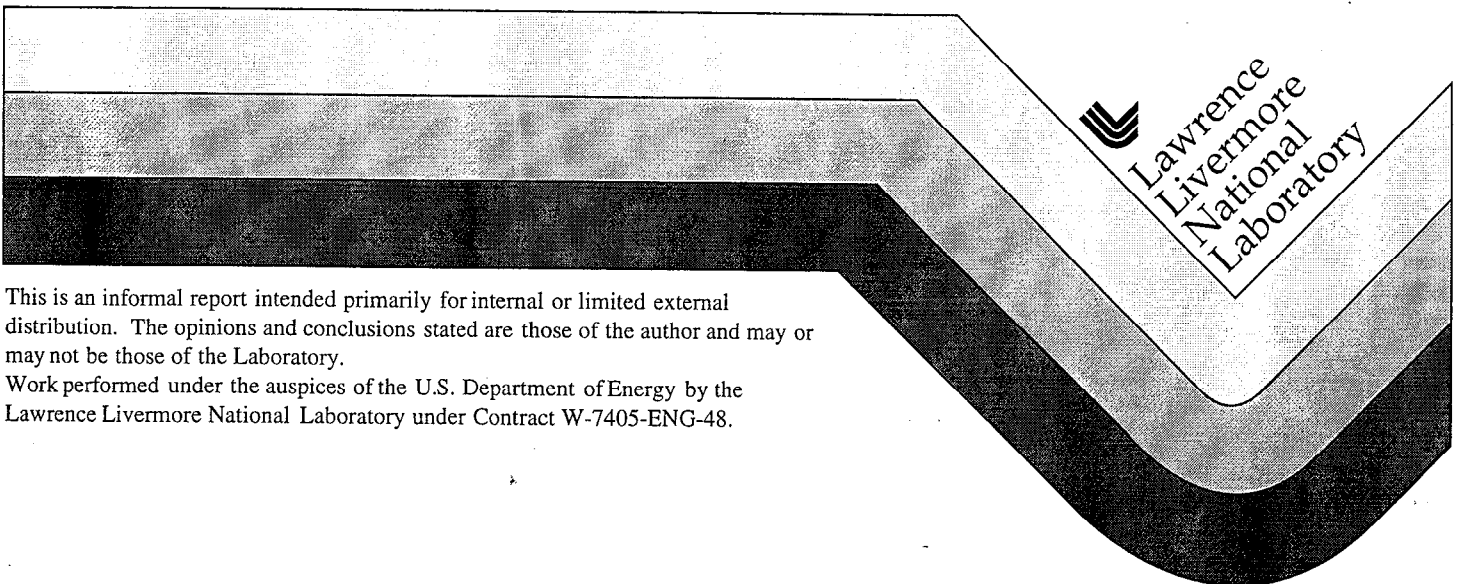


Recent Applications of Bandpass Filtering

M. D. Denny

March 15, 1999



This is an informal report intended primarily for internal or limited external distribution. The opinions and conclusions stated are those of the author and may or may not be those of the Laboratory.

Work performed under the auspices of the U.S. Department of Energy by the Lawrence Livermore National Laboratory under Contract W-7405-ENG-48.

DISCLAIMER

This document was prepared as an account of work sponsored by an agency of the United States Government. Neither the United States Government nor the University of California nor any of their employees, makes any warranty, express or implied, or assumes any legal liability or responsibility for the accuracy, completeness, or usefulness of any information, apparatus, product, or process disclosed, or represents that its use would not infringe privately owned rights. Reference herein to any specific commercial product, process, or service by trade name, trademark, manufacturer, or otherwise, does not necessarily constitute or imply its endorsement, recommendation, or favoring by the United States Government or the University of California. The views and opinions of authors expressed herein do not necessarily state or reflect those of the United States Government or the University of California, and shall not be used for advertising or product endorsement purposes.

This report has been reproduced
directly from the best available copy.

Available to DOE and DOE contractors from the
Office of Scientific and Technical Information
P.O. Box 62, Oak Ridge, TN 37831
Prices available from (615) 576-8401, FTS 626-8401

Available to the public from the
National Technical Information Service
U.S. Department of Commerce
5285 Port Royal Rd.,
Springfield, VA 22161

Recent Applications of Bandpass Filtering

Abstract

Bandpass filtering has been applied recently in two widely different seismic applications: S.R. Taylor and A.A. Velasco in their source-path amplitude-correction (SPAC) algorithm and N.K. Yacoub in his maximum spectral energy algorithm for picking teleseismic P-wave arrival times. Though the displacement spectrum is the intermediate product in both cases, the filters and scaling corrections used to estimate it are entirely different. We tested both and found that the scaling used by Taylor and Velasco worked in all cases tested whereas Yacoub's did not. We also found that bandpass filtering as implemented by Taylor and Velasco does not work satisfactorily; however, the Gaussian filter used by Yacoub does work. The bandpass filter of Taylor and Velasco works satisfactorily when the results are centered in the band; however, a comb filter with the same number of poles and zeroes as the bandpass used by Taylor and Velasco works better than the bandpass filter.

Introduction

Bandpass filtering, after years of being overshadowed by the fast Fourier transform (FFT), is enjoying renewed popularity for use in seismic signal processing. Researchers at Los Alamos National Laboratory (LANL) are currently using it in their SPAC algorithm (Taylor and Velasco, 1998) for characterizing seismic events. In another form, Yacoub (1998) is using bandpass filtering in his maximum spectral energy technique for picking teleseismic P-wave arrival times. In both of these algorithms, accurate estimates of spectral amplitudes are crucial to the final application, yet the filters applied in these two cases are as different as the approaches employed to scale the filtered time series. Ironically, these diverse implementations are occurring at a time when a strong drive to standardize processing techniques exists within the Comprehensive Test Ban Treaty (CTBT) monitoring community so that the same concerns are not raised repeatedly. With a view toward standardizing on one technique, not necessarily either of the two mentioned above, we have evaluated both approaches along with some alternatives.

Background

In the SPAC signal-processing algorithm, the objective is to model the seismic-source function

and the attenuation along the propagation path. For this application, a simple yet accurate procedure for estimating the signal's displacement spectrum is needed. The first step in the procedure adopted for SPAC is to filter the signal, as recorded in velocity, with a set of eight filters that are more or less logarithmically spaced over the interval of 0.5 to 6.0 Hz. Each of these filters is a zero-phase, Butterworth bandpass filter that is one octave wide with four poles. The final steps are to compute the root-mean-square (RMS) value of each of the filtered time-series and then to convert them to a spectral displacement by dividing by $\omega(2\pi f)$ and multiplying by a scaling parameter derived from Parseval's theorem. The scaling parameter is

$$\sqrt{\frac{T}{E}}, \quad (1)$$

where T is the length of the signal, and E is the total energy in a filter's bandpass. In this case, the total energy of the filter is approximately twice the bandwidth. The final results are assigned to the low-frequency corner (low-cut) of each of the bandpass filters in an attempt to account for the possibility that the high-frequency decay (roll-off) of the signal could result in the RMS amplitudes being biased high relative to the log-averaged frequency-domain amplitudes.

In the maximum spectral energy algorithm, the objective is to measure a reliable arrival-time for

a teleseismic P-wave and to use this arrival to locate the event. The procedure advocated by Yacoub (1998) is to pass the signal, converted to displacement with the recording instrument response removed, through a set of Gaussian filters and then to compute the envelopes of the filtered traces. The Gaussian filtered is given by

$$e^{-\alpha \left(\frac{f}{f_c} - 1 \right)^2}, \quad (2)$$

where α is an arbitrary constant, chosen by Yacoub to be 50, and f_c is the corner frequency. Eight filters are used and are uniformly spaced 0.1 Hz apart from 0.7 to 1.4 Hz. The filtered traces are scaled by (i.e., divided by) the maximum amplitude of the impulse response of each filter, given by Herrmann (1973) as

$$f_c \sqrt{\pi/\alpha}, \quad (3)$$

The envelopes are compared, and the one with the largest amplitude in a predetermined window is chosen. The time to this peak is the quantity used in a location algorithm.

Scaling

We begin by addressing the scaling question. We use a simple second-order source generated by passing a unit impulse through a causal second-order, Butterworth, low-bandpass filter. To this signal, we add random noise and compare the results of scaling by the two methods discussed above. Next, the composite signal and noise are both filtered using the Gaussian filter and scaled by the two techniques described above. The results are shown in Figure 1 for two cases (2 to 1 and 10 to 1) of signal-to-noise ratio (SNR). For the composite signal, the two techniques yield comparable results. However, for the case of noise alone, the Herrmann technique is seen to grossly underestimate the known spectra.

The above results are not unexpected. The Herrmann technique was derived to analyze surface waves, which are relatively simple compared to noise. In fact, surface waves have the same deterministic property that our simple pulse has; that is, each point is related to the previous ones in a well-defined way. Thus, the expectation is that a single measure of the filtered trace is representative of the energy in the total signal. On the other hand, this is not

the expectation for a random signal such as noise. It is, therefore, unreasonable to apply Herrmann scaling to any complex signals for which the next point is not determined by the previous ones. This consideration also applies to a signal composed of multiple wavelets. In this case, although the multiple wavelets can be considered to have a common source, they can also be considered to have a Green's function, which is essentially random in amplitude and in delay times between arrivals. We conclude that, in general, the scaling constant derived from Parseval's theorem should be used.

Bandwidth

As noted above, Taylor and Velasco (1998) assign the final spectral estimate to the low-cut frequency of the bandpass filter to offset any bias that might be due the roll-off of the signal. To test the validity of this procedure, we use four sources that differ only in roll-off. We assess the error when the RMS value of the filtered time-series is assigned to the low-cut corner and, in another case, when it is assigned to the mean of the high- and low-cut corners of the bandpass filter. At the same time, we assess the merit of choosing to represent the signal in velocity instead of displacement as in the Yacoub technique. We elected to include acceleration in the test for completeness; consequently, we evaluated 24 cases.

The results of our tests are given in Table 1, and the full set of filtered traces is reproduced in the Appendix. Table 1 shows that attributing the result to the center frequency is the best choice by a large margin. However, the choice of physical representation is less obvious. The table shows the maximum errors when working in acceleration are essentially constant, at least up to a roll-off of 4, because they occur below the corner frequency, whereas the maximum errors from working in displacement all occur at frequencies above the corner frequency and increase with increasing roll-off. The maximum errors for velocity, however, are not as consistent as the centered case. For roll-offs of 3 or less, the maximum errors all occur below the corner frequency; whereas, for a roll-off of 4, the maximum error occurs above the corner frequency. However, we note that the maximum errors exceed those from working in acceleration only when the roll-off is greater than 4, and that they

are only slightly larger than those from working in displacement when the roll-off is 2 or smaller. Furthermore, they are less when the roll-off is greater than 2. Therefore, when large amounts of data need to be processed in a consistent manner, representing the signal in velocity is a good choice.

The choice of representation, however, should be made to whiten (i.e., flatten) the pre-event noise spectrum. Doing so alleviates some of the concerns that led LANL to assign the result to the low-cut corner. That is, at frequencies for which the signal-to-noise ratio is low, high noise outside the band of interest can bias the resulting estimate high. In such cases, a Gaussian or a comb filter (Streans, 1975) is a better choice than a one-octave bandpass filter. The reason for this is that both of these filters severely reduce the out-of-band (outside the half-power points) contribution and emphasize the energy at a single frequency (Figure 2). These filters leave little doubt as to where the result should be assigned. In fact both filters out-perform the bandpass filter in terms of error as shown in Table 2. The filtered traces from which the results in this table are derived are shown for reference in the Appendix.

Summary

We have demonstrated, by using specific examples, that scaling is best done in the random signal case by applying Parseval's theorem. We have also shown that a comb filter, which is no more complex than the bandpass filter, results in smaller errors by nearly a factor of 2. We have further demonstrated that the Gaussian filter yields comparable results to the comb filter for an α of 20.

References

- Herrmann, R.B. (1973), "Some aspects of band-pass filtering of surface waves," *Bul. Seis. Soc. Am.* **63**(2), 663-671.
- Taylor, S.R., and A.A. Velasco (1998), *User's manual for SPAC 1.0: a MatLab program for computing source and path amplitude corrections*, Los Alamos National Laboratory, Los Alamos, NM, LAUR-98-4363.
- Yacoub, N.K. (1998), *Maximum spectral energy for locating seismic events*, Presentation to the AFTAC Seismic Review Panel, June 1998.
- Stearns, S.D. (1975), *Digital signal analysis*, Hayden Book Company, Inc., Rochelle Park, NJ.

Table 1. Bandpass filter maximum errors (%). NOTE: The letters L and H mean the maximum error occurs on the low or the high side of the corner frequency, respectively.

Roll-off	LANL			Center		
	Acceleration	Velocity	Dissipation	Acceleration	Velocity	Dissipation
-1	142 L	50 L	27 H	22 L	7 L	1 H
-2	147 L	53 L	46 H	23 L	8 L	6 H
-3	174 L	53	56 H	24 L	8 L	21 H
-4	147 L	56 H	63 H	24 L	21 H	45 H

Table 2. Comb and Gaussian filter maximum errors (%).

Roll-off	Comb			Gauss		
	Acceleration	Velocity	Dissipation	Acceleration	Velocity	Dissipation
-1	12 L	3 L	0	3 L	0	1 H
-2	13 L	4 L	4 H	3 L	1 H	6 H
-3	13 L	4 L	13 H	3 L	6 H	15 H
-4	13 L	13 H	28 H	6 L	15 H	29 H

Recent Applications of Bandpass Filtering

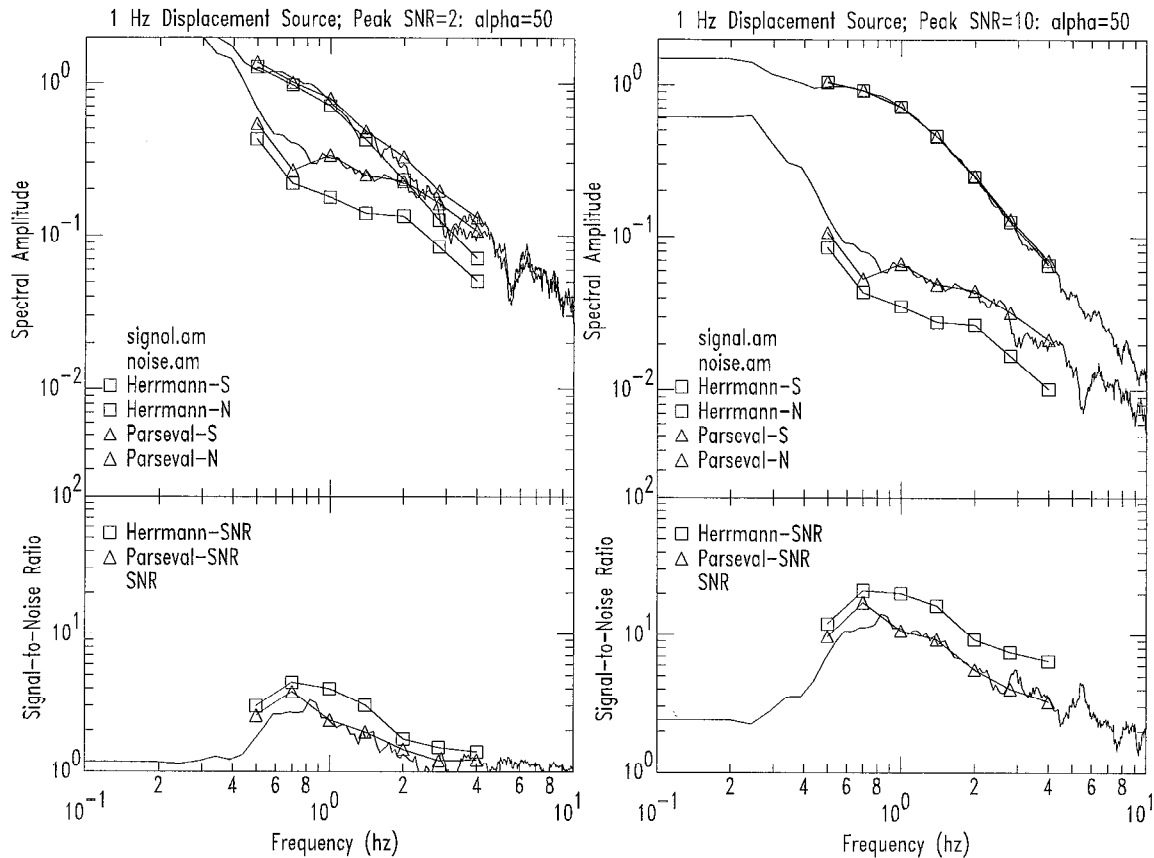


Figure 1. Comparison of scaling factors. Both Herrmann scaling and one derived from Parseval's theorem work well in the case for which the maximum SNR is 10. In the case for which the maximum SNR was specified as 2, however, Herrmann scaling does not work as well. In both SNR cases, Herrmann scaling grossly underestimates the noise spectrum. As explained in the text, this is to be expected. Gaussian filters were used in this example.

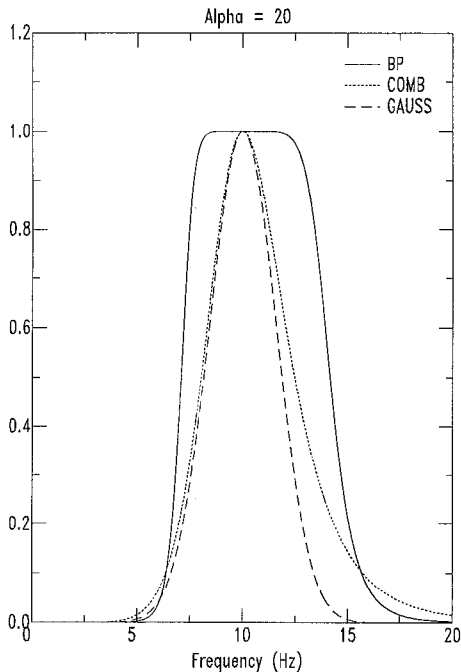


Figure 2. Bandpass comparisons. The comb filter shown is the same order as the bandpass filter but consists of a low-pass followed by a high-pass filter; both filters have the same corner frequency. For the Gaussian filter, the parameter α was chosen so that its maximum errors would be comparable to the errors of the comb filter. As shown, this requirement results in the Gaussian filter having approximately the same low-frequency decay as the comb filter.

Appendix: Filtered Traces

The displacement source functions used in the test results shown in the following figures are the unit impulse responses of Butterworth low-pass filters of orders 1, 2, 3, and 4, respectively. The corner frequency in all cases is 2.24 Hz and was chosen to be logarithmically half way between the lowest and the highest of the sampled frequencies. The velocity and acceleration functions were created simply by differentiating once and twice, respectively. In each of the figures, the displacement and velocity spectra are plotted on the left-hand side of the page, and the acceleration and the errors associated with all three are plotted on the right-hand side. The error is shown as the ratio of the estimated to the actual.

Figures 1.1 through 2.4 show the results obtained from one-octave bandpass filters. In **Figures 1.1 through 1.4**, the results of assigning the scaled-RMS values to the low-cut frequency of the bandpass filter are shown, and the improvements that result from assigning the scaled RMS values to the center of the bandpass are demonstrated in **Figures 2.1 through 2.4**.

The results of applying a set of comb filters are shown in **Figures 3.1 through 3.4**, and the results from a Gaussian filter are shown in **Figures 4.1 through 4.4**.

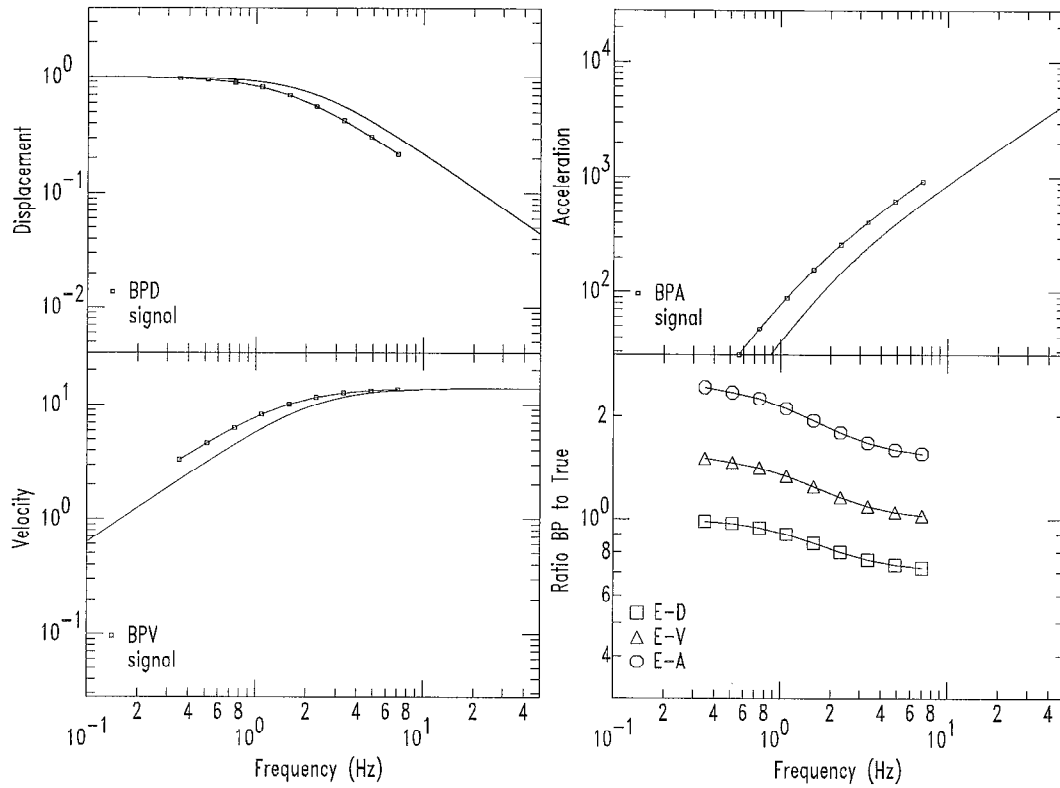


Figure 1.1

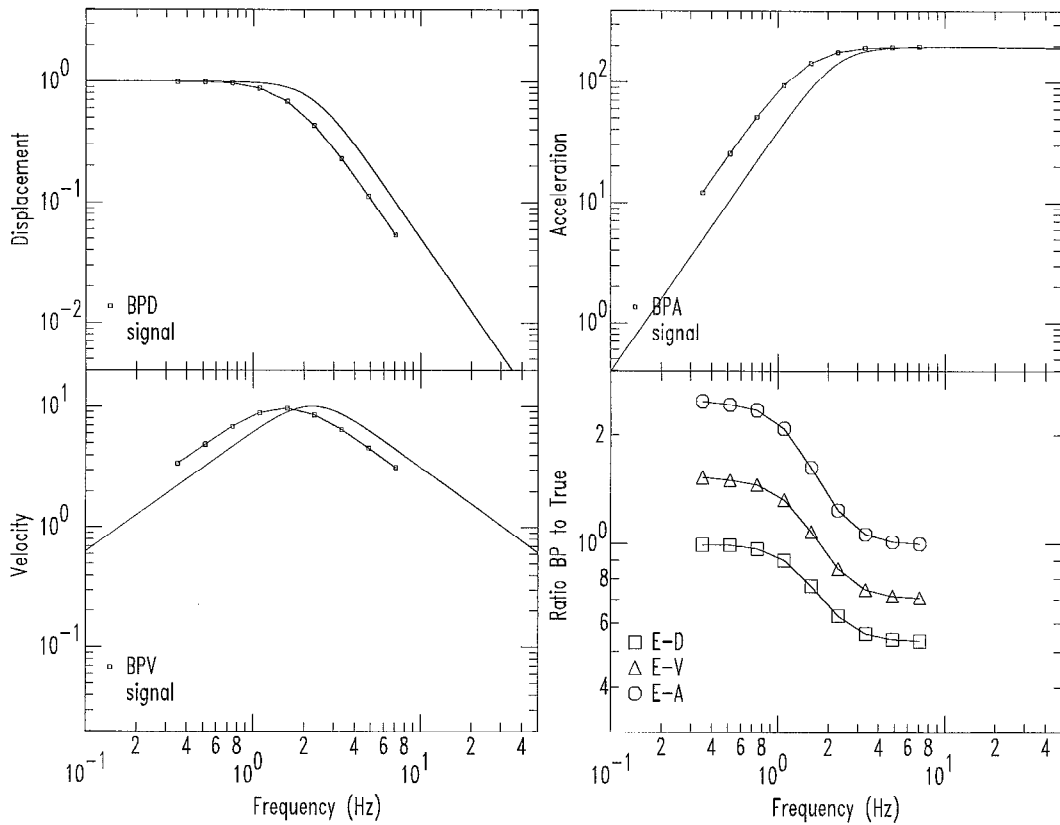


Figure 1.2

Recent Applications of Bandpass Filtering

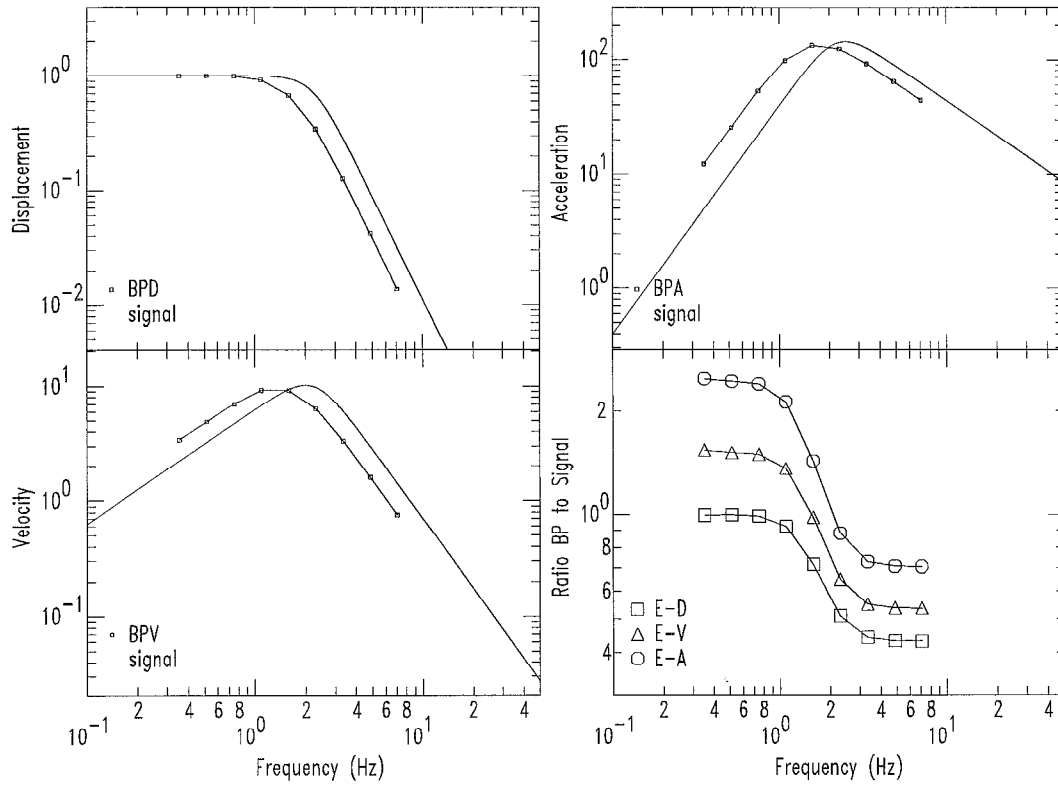


Figure 1.3

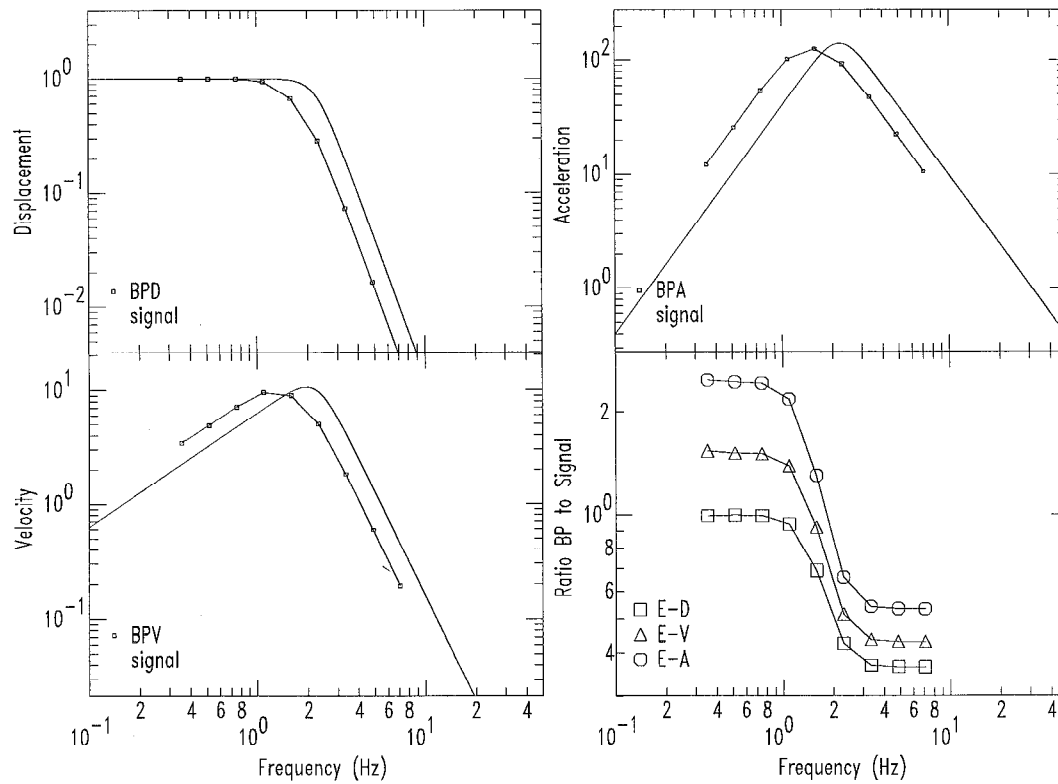


Figure 1.4

Recent Applications of Bandpass Filtering

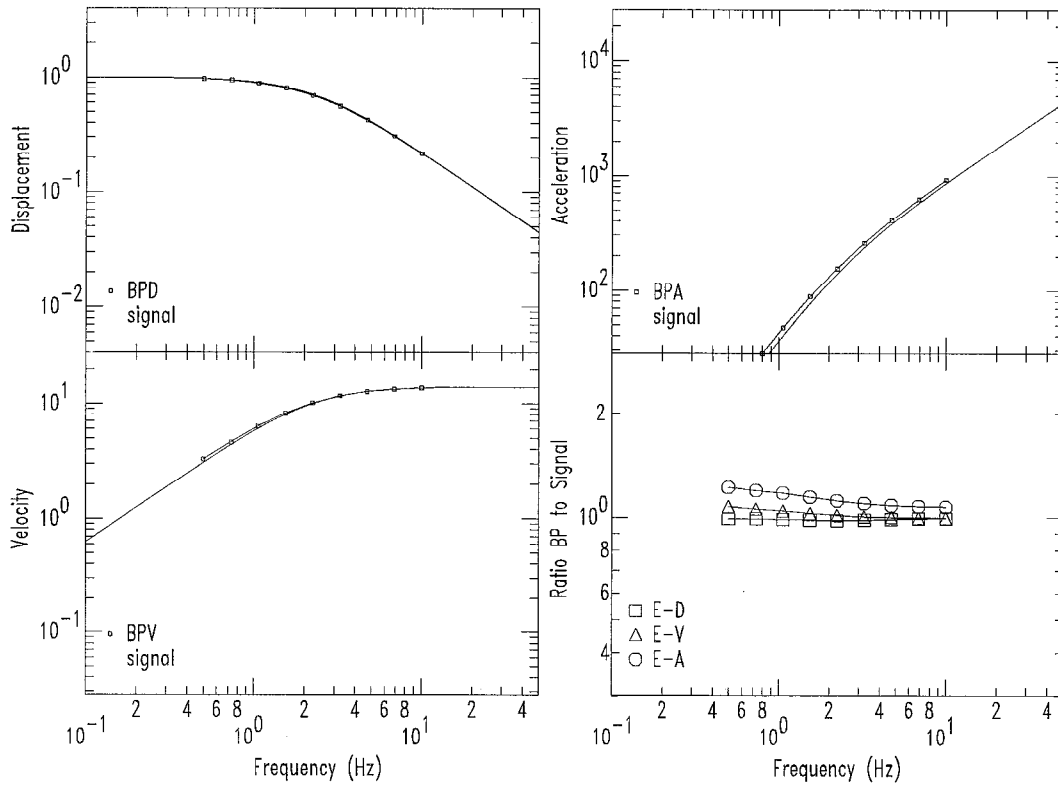


Figure 2.1

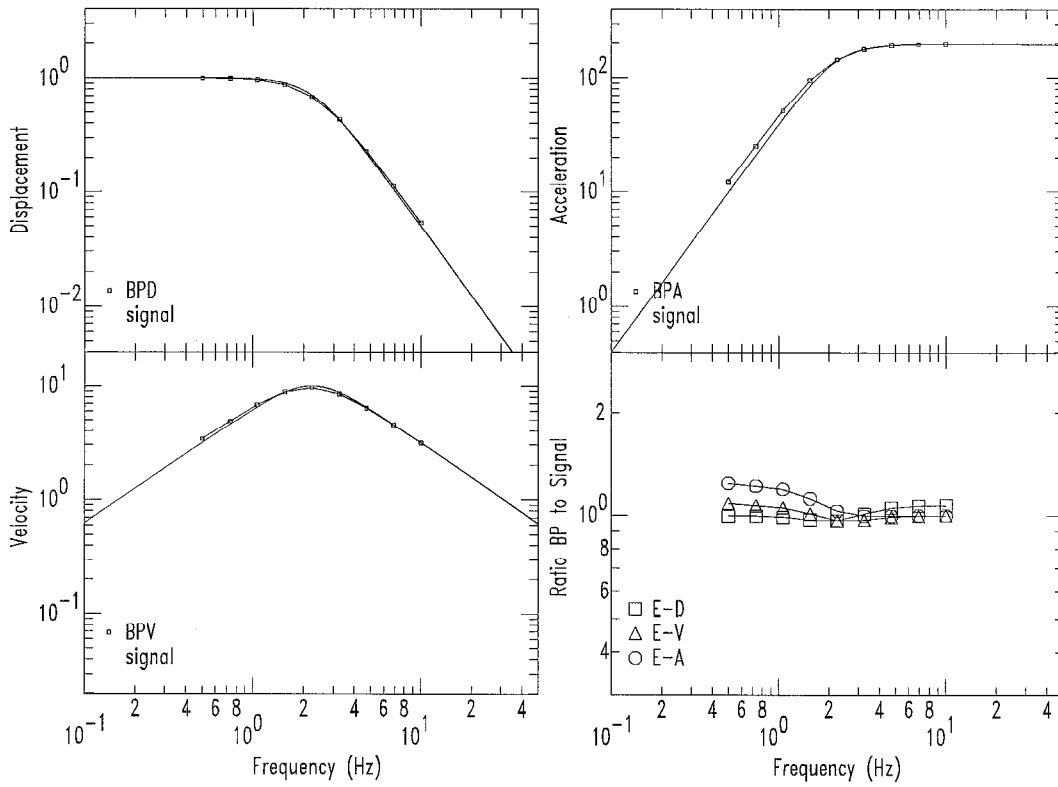


Figure 2.2

Recent Applications of Bandpass Filtering

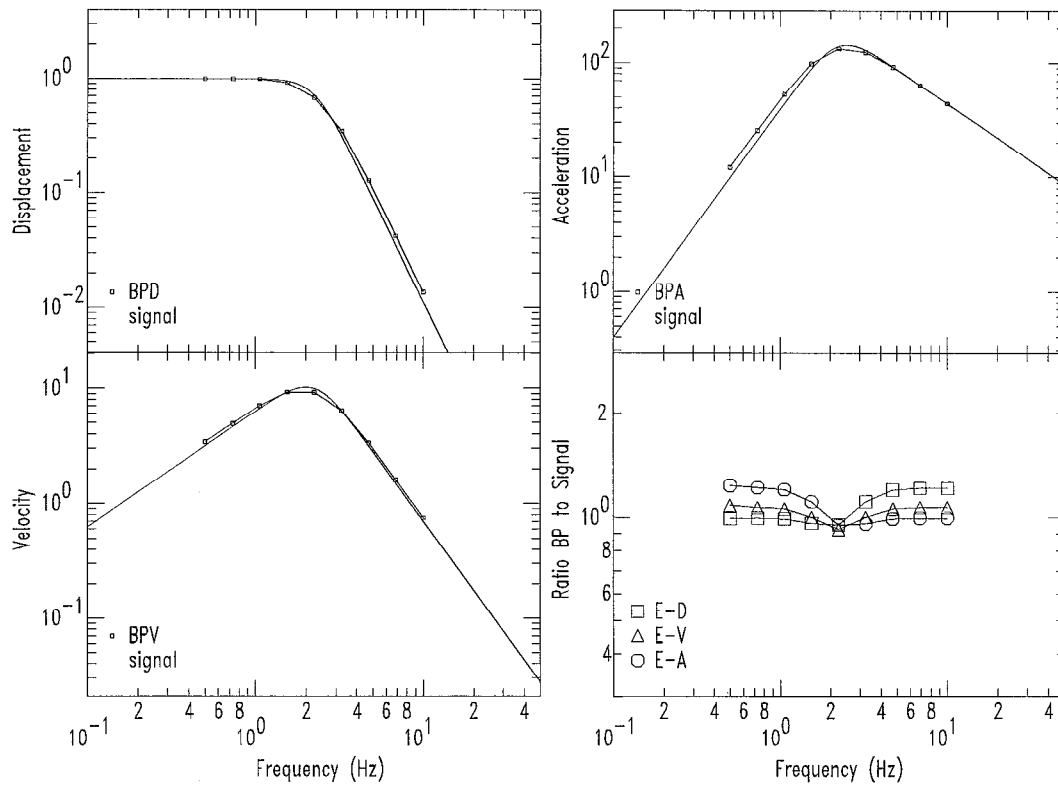


Figure 2.3

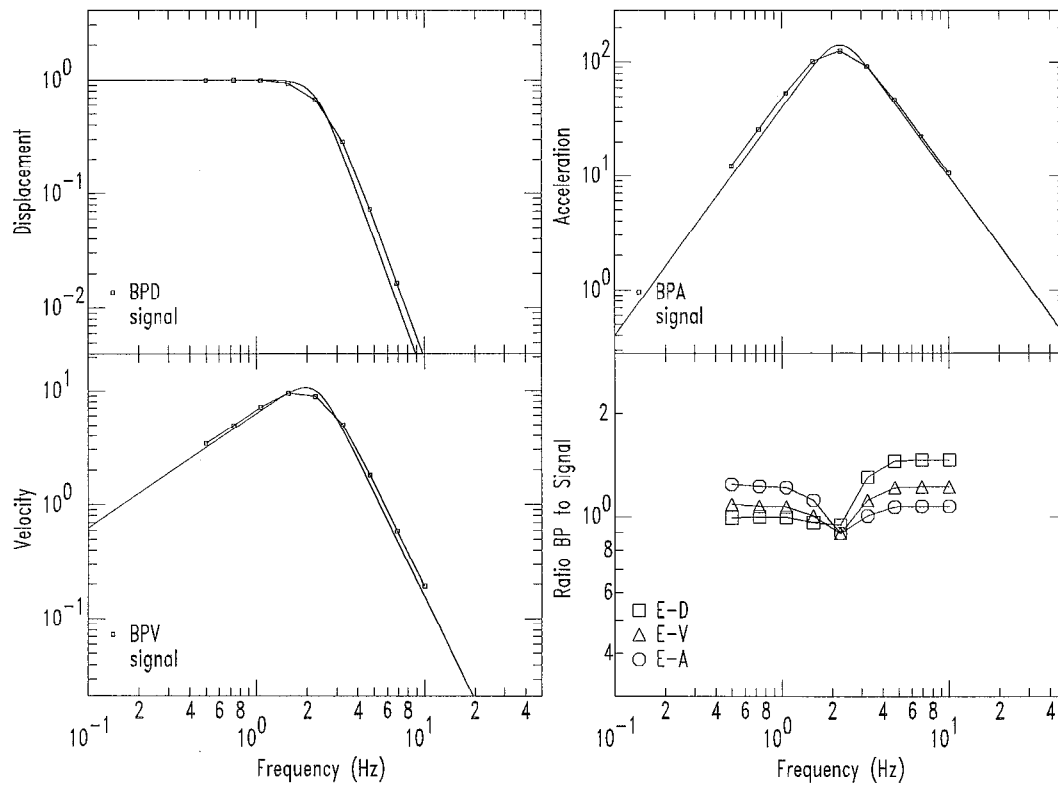


Figure 2.4

Recent Applications of Bandpass Filtering

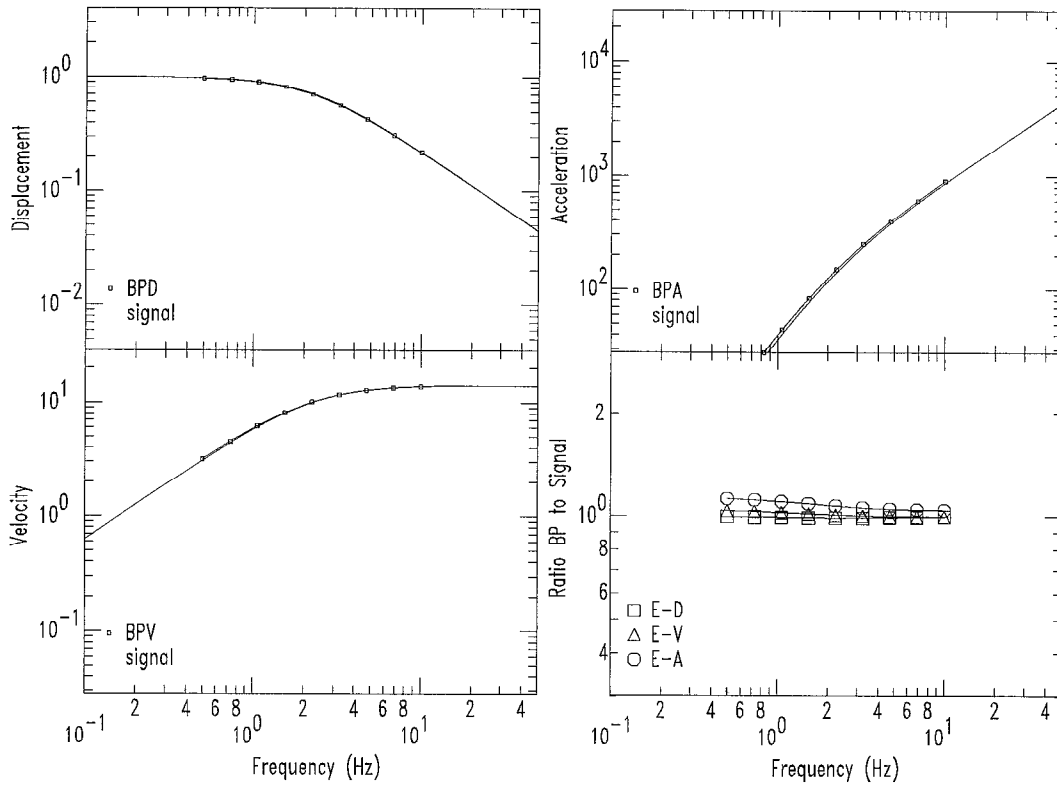


Figure 3.1

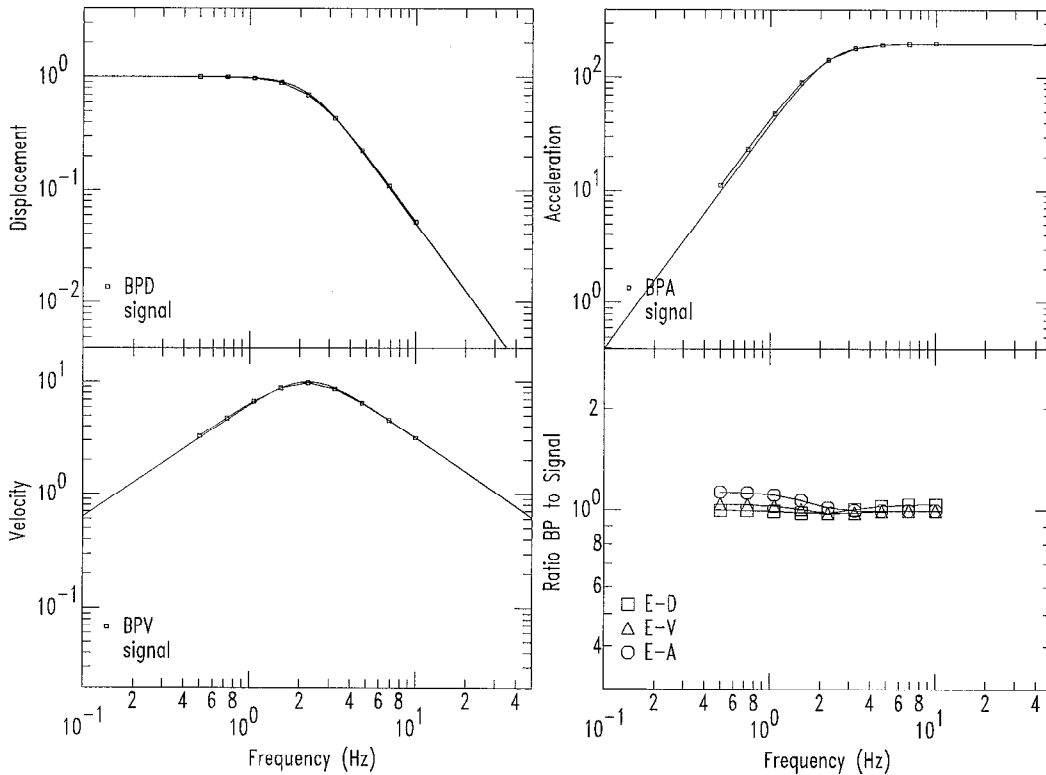


Figure 3.2

Recent Applications of Bandpass Filtering

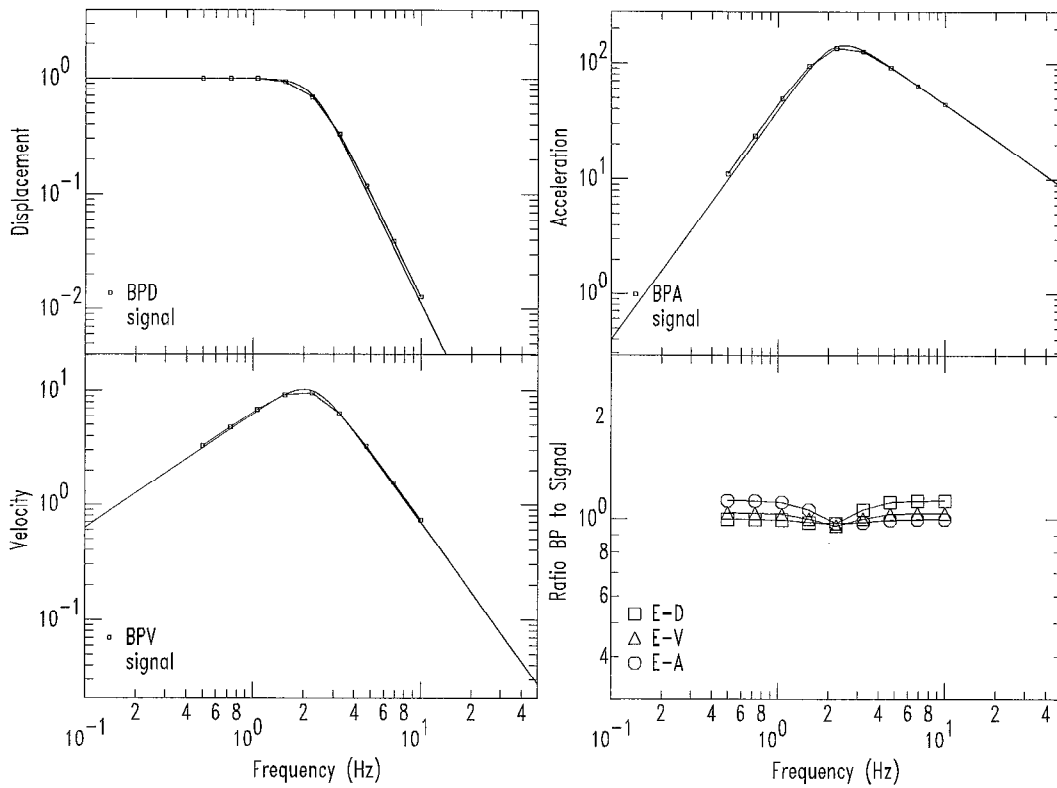


Figure 3.3

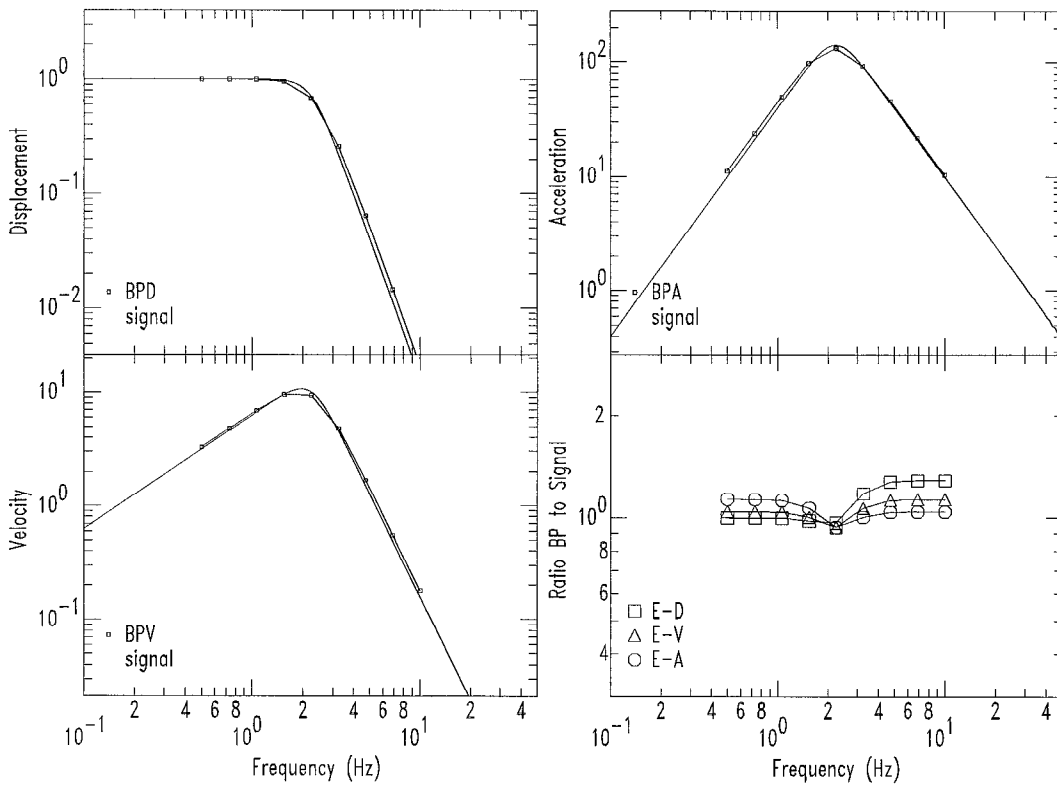


Figure 3.4

Recent Applications of Bandpass Filtering

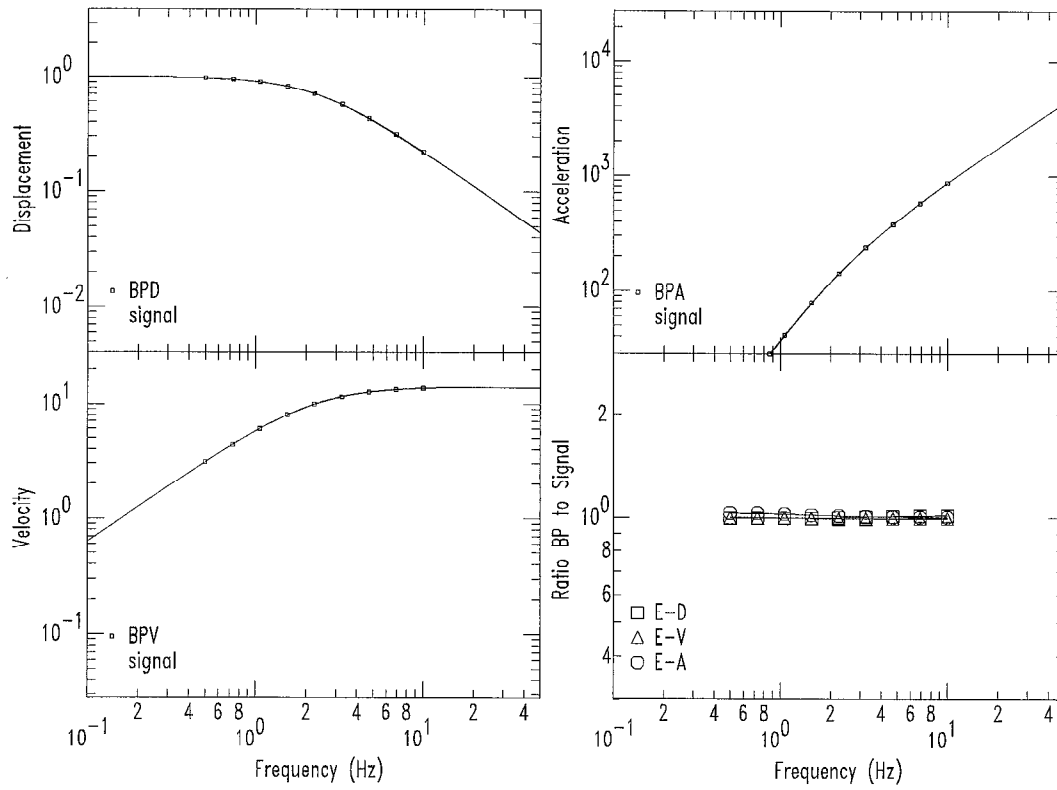


Figure 4.1

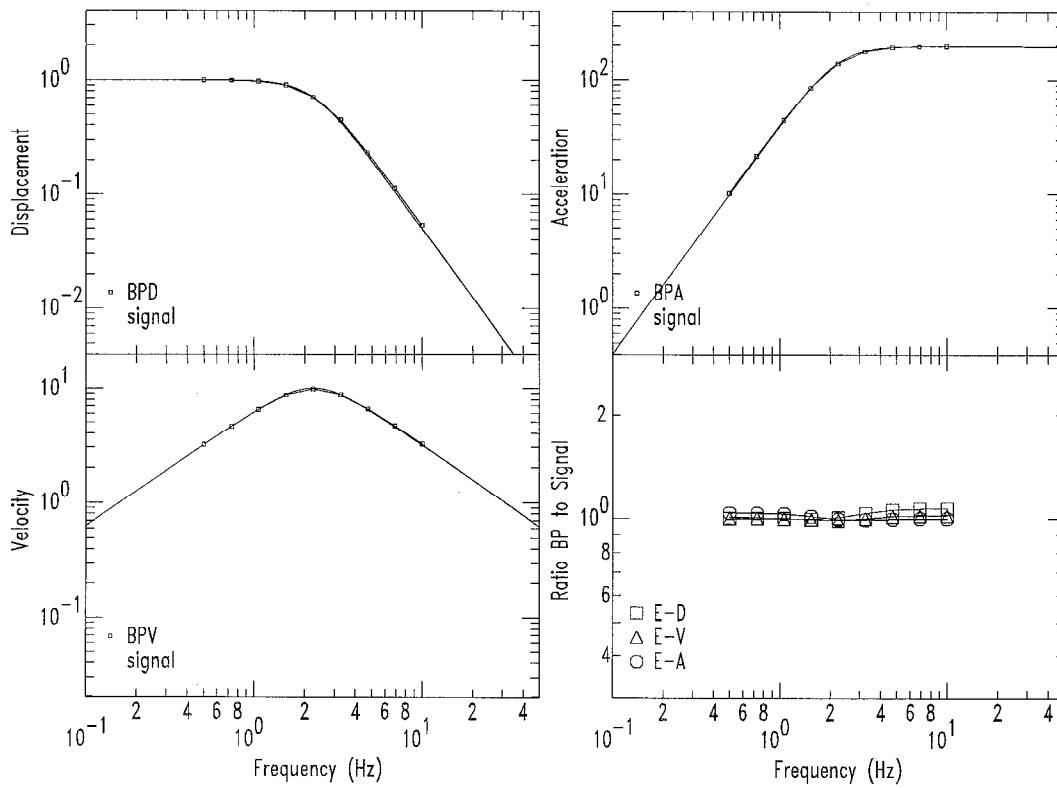


Figure 4.2

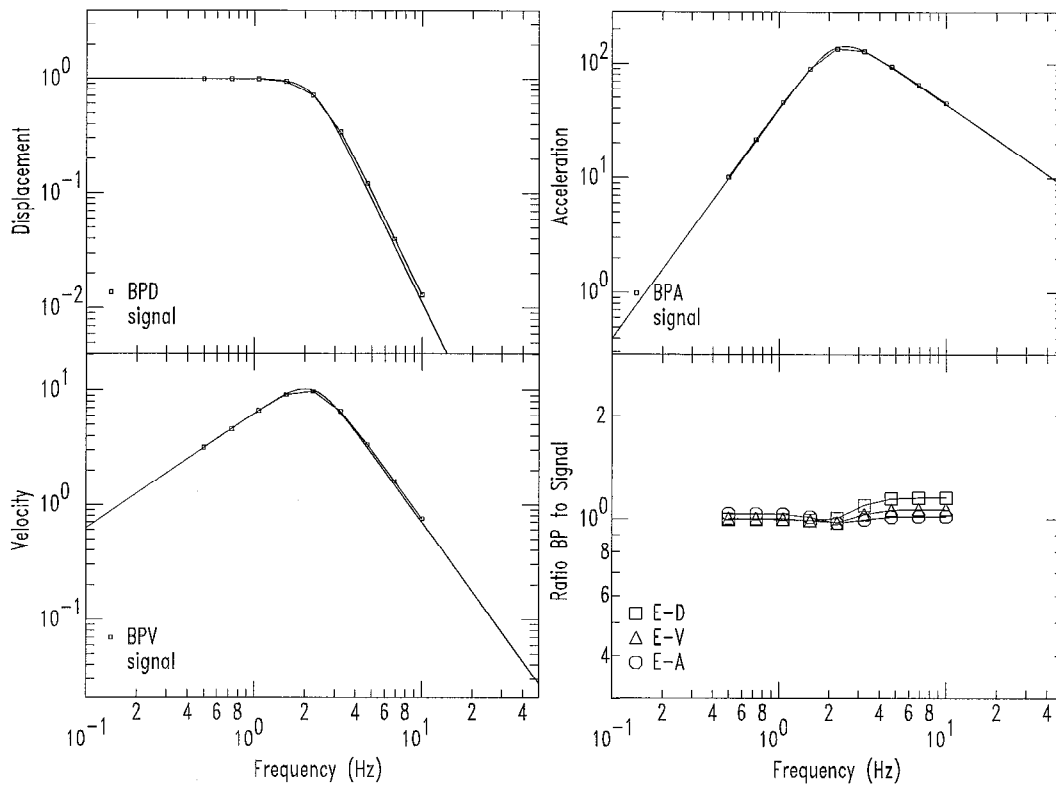


Figure 4.3

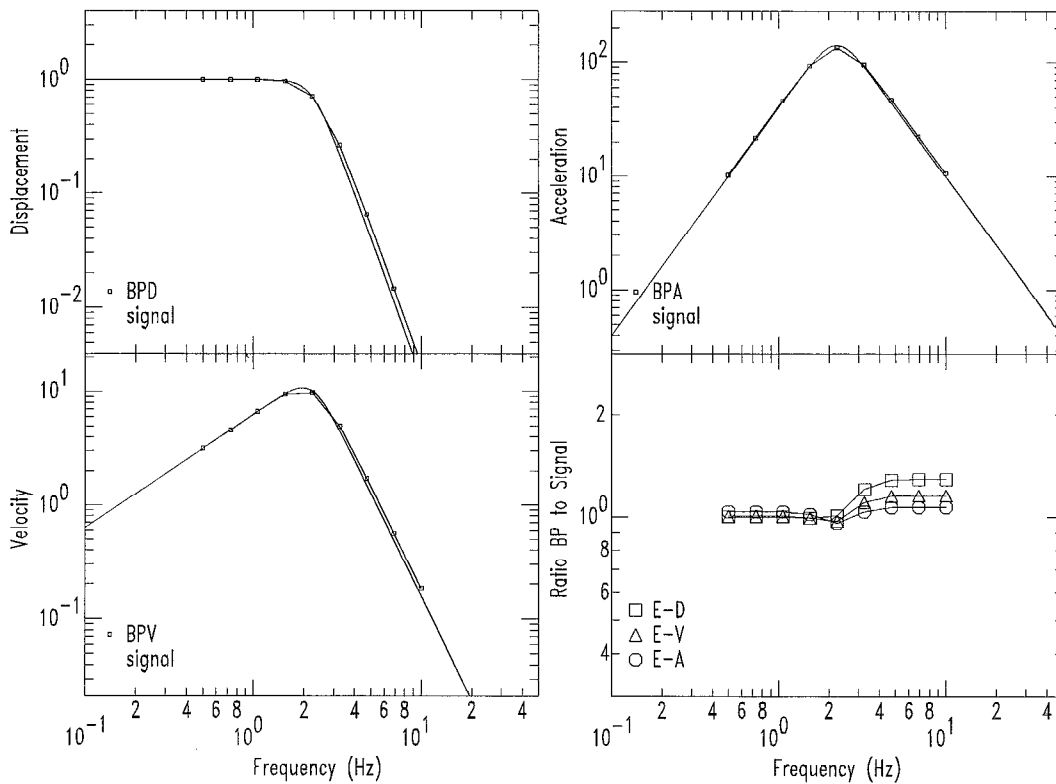


Figure 4.4